Article

Poly(methylvinylsiloxane)-Based High Internal Phase Emulsion-Templated Materials (polyHIPEs)—Preparation, Incorporation of Palladium, and Catalytic Properties

Jan Mrówka, Mariusz Gackowski, Lidia Lityńska-Dobrzyńska, Andrzej Bernasik, Robert Kosydar, Alicja Drelinkiewicz, and Magdalena Hasik*

Cite This: *Ind. Eng. Chem. Res.* 2020, 59, 19485−19499

Read Online

ACCESS | Metrics & More | Article Recommendations | SI Supporting Information

ABSTRACT: Poly(methylvinylsiloxane) (V_3 polymer) obtained by kinetically controlled anionic ring-opening polymerization of 1,3,5-trimethyl-1,3,5-trivinylcyclotrisiloxane was cross-linked with various amounts of 1,3,5,7-tetramethylcyclotetrasiloxane (D_4^H) in w/o high internal phase emulsions (HIPEs). PolyHIPEs thus prepared differed in the polymer cross-linking degree, which affected their porous morphology and total porosity. The obtained V_3 polymer-based polyHIPEs were applied as matrices for the incorporation of Pd from the $Pd(OAc)_2$ solution in tetrahydrofuran. This process involved the conversion of Si−H groups remaining in the polymer networks and resulted in the formation of crystalline, metallic Pd in the systems. Mean sizes of the generated Pd crystallites were lower in polyHIPEs of higher than in those of lower polymer cross-linking degrees and porosities (∼5 nm *vs* ∼8 nm, respectively). The Pd-containing polyHIPEs showed activity in catalytic hydrogenation of the triple carbon−carbon bond in phenylacetylene giving the unsaturated product, styrene with a selectivity of ca. 80%. To the best of our knowledge, this is the first work devoted to polysiloxane-based polyHIPEs with dispersed metallic particles.
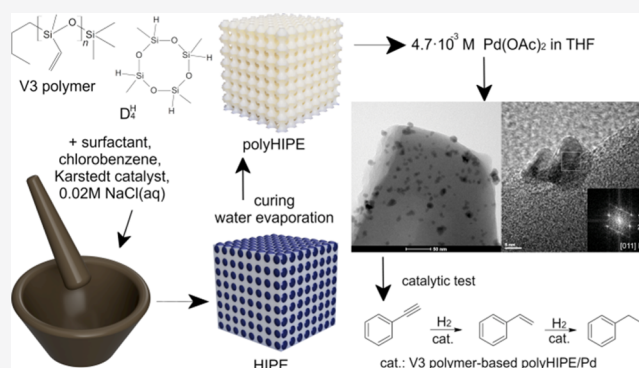
1. INTRODUCTION

Porous solids are widespread and play important roles in nature. There are also common (e.g., ceramics, cements) as well as more sophisticated man-made porous materials (e.g. ordered mesoporous silica[1] and organosilicas,[2] metal−organic frameworks—MOFs,[3] covalent organic frameworks[4]) of well-established or potentially, valuable applications. Porous synthetic polymers are, however, a special group of materials because they combine advantageous properties inherent to both porous structures (accessibility) and macromolecular compounds (good processability, ease of functionalization).

There are various ways to fabricate pores in polymers; the most attractive ones that allow the precise control of shapes and sizes of the cells formed make use of templates.[5] In particular, high internal phase emulsion (HIPE) templating is the method which leads to the preparation of macroporous polymers. In its original version, patented in 1982,[6] HIPE templating involves radical copolymerization of vinyl co-monomers (styrene and divinylbenzene or styrene, butyl methacrylate and allyl methacrylate) in a water-oil (w/o) emulsion stabilized by a suitable surfactant. Co-monomers and surfactants form the external (continuous) phase of the emulsion, whereas the internal (dispersed) aqueous phase constitutes at least 74% of the whole emulsion volume.

Because one of the co-monomers is difunctional, the process results in the polymer network grown around the internal phase droplets. Removal of the internal phase from the copolymerization product leaves behind the porous structure, called polyHIPE, that replicates internal phase dispersion in the emulsion.

Since their first description, polyHIPEs synthesized *via* conventional radical copolymerization of styrene and divinylbenzene in w/o emulsions have been the focus of numerous studies.[7−11] However, other monomers, polymerization methods, and/or types of emulsion have been used in HIPE templating as well. For example, ring-opening copolymerization of ε-caprolactone and a difunctional monomer (4,4-bioxepanyl-7,7′-dione) in oil-oil (o/o) HIPE has led to macroporous polyesters showing the shape memory effect.[12] Step-growth polymerization of formaldehyde and melamine in

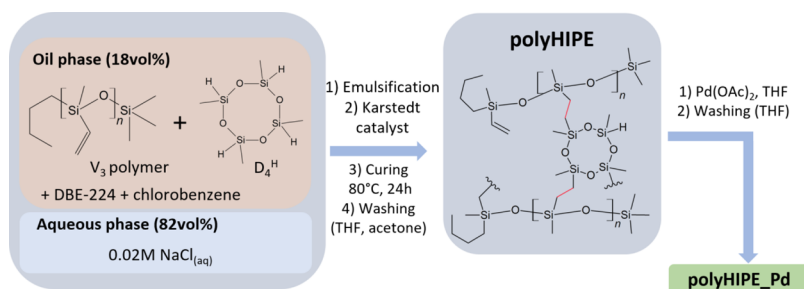**Scheme 1. Strategy for the Preparation of the Materials Studied in the Work**

HIPE with paraffin oil as the dispersed phase and mixed DMSO−H$_2$O solvent added to the continuous phase has resulted in polyHIPE materials exhibiting potential for application as CO$_2$ absorbents.[13] Ring-opening metathesis polymerization (ROMP) of dicyclopentadiene[14] or one of the controlled radical polymerization methods, namely, reversible addition-chain-transfer polymerization (RAFT) of styrene and divinylbenzene[15] in w/o HIPE, has brought about polyHIPEs of enhanced mechanical properties. Novel ideas in the field of polyHIPEs include the use of biomass-based monomers: vanillin and lauryl methacrylates[16] and a monomer acting simultaneously as a HIPE stabilizer (a block copolymer tetrol)[17] in the preparation of macroporous methacrylate copolymers (by radical copolymerization in w/o HIPE, with divinylbenzene cross-linker) and polyurethanes (by step-growth polymerization in o/o HIPE, with polyisocyanate as the second monomer), respectively. Currently, an interest in functionalization of polyHIPEs aimed at tuning their properties for given applications is observed. Thus, for example, recently polyHIPEs with introduced 12-crown-4 ether groups have been demonstrated to be perfectly suited for selective Li$^+$ ion capture from aqueous solutions.[18]

It should be noted that most of polyHIPEs studied so far have been obtained using organic compounds. There are only a few reports which deal with the polyHIPEs prepared from organosilicon compounds containing Si−O bonds in their structure or with incorporated moieties of such compounds. Grosse et al.[19] have shown that macrocellular polysiloxane networks can be formed when polyhydromethylsiloxane (PHMS) is cross-linked *via* the so-called hydrosilylation reaction, that is, the catalytic addition of Si−H groups in PHMS to vinyl groups in 1,3-divinyltetramethyldisiloxane or 1,3,5,7-tetramethyl-1,3,5,7-tetravinylcyclotetrasiloxane, carried out in w/o HIPE. Normatov and Silverstein in a series of papers[20−22] have described organic−inorganic polyHIPEs based on 2-ethylhexylacrylate and silsesquioxanes. Incorporation of silsesquioxane units influenced mechanical and thermal properties of the systems.

In recent years, our group has been involved in the studies of polysiloxane[23−25] and polysiloxane-silazane[26] networks prepared by hydrosilylation or functionalization of siloxanes[27] using the hydrosilylation process. We have found that the polysiloxane networks formed by this method are capable of reducing to metallic forms Pd^{2+}[28] and Pt^{4+}[29] ions present in tetrahydrofuran (THF) solutions of palladium(II) acetate (Pd(OAc)$_2$) and PtCl$_4$, respectively. The systems with introduced Pt particles have been tested as catalysts in isopropyl alcohol conversion.[29]

Polysiloxane networks studied by us previously were glassy, nonporous solids. For metal incorporation and in catalytic applications, however, the use of porous supports may be advantageous. In catalysis, macropores present in the carrier facilitate fast migration of the reagents and the products from catalytically active sites, whereas meso/micropores ensure a large specific surface area for the adsorption ability.[30] Pore sizes and size distributions can control the sizes and size distributions of metal particles formed on the porous support as well as may contribute to their good dispersion by preventing them from sintering.[30] All these features are crucial for achieving high catalyst activity. Therefore, we decided to extend our earlier investigations. Thus, in the present work porous networks were obtained by cross-linking of poly-(methylvinylsiloxane), here on referred to as V$_3$ polymer, with 2,4,6,8-tetramethylcyclotetrasiloxane (D$_4^H$) in w/o HIPE. The prepared networks differed in the polymer cross-linking degree as well as in the porous structure and porosity. Then, they were treated with Pd(OAc)$_2$ solution in THF. Finally, catalytic hydrogenation of phenylacetylene (PhAc) in the presence of the thus formed polysiloxane—Pd composites was carried out. The overall strategy for the preparation of the studied materials is presented in Scheme 1.

To the best of our knowledge, this is the first study devoted to the preparation of siloxane polyHIPEs with dispersed metallic particles. The reports on the incorporation of metals into other polyHIPEs are not numerous, either. In particular, palladium was introduced to polyHIPEs based on the polystyrene−divinylbenzene copolymer,[31] styrene−vinylbenzyl chloride−hexanedioldiacrylate copolymer functionalized by amine, ethylenediamine or ammonium groups,[32] and organo-silicas.[33,34] The Pd-containing systems were applied as catalysts of allyl alcohol hydrogenation,[31] Suzuki−Miyaura,[32] and Mizoroki−Heck[34] coupling reactions. It should be noted that because of the advantageous properties of polysiloxanes as compared with organic polymers, especially their high thermal stability, catalysts supported on HIPE-templated polysiloxanes can be applied in wider temperature ranges than those with carbon-based polyHIPEs serving as carriers. Therefore, the results presented in this work may pave the way for the design of new systems containing catalytic centers dispersed in polyHIPEs derived from polysiloxanes, suitable for use in various chemical processes, including those requiring high temperatures.

2. EXPERIMENTAL SECTION

2.1. Materials. The V$_3$ polymer was prepared by kinetically controlled anionic ring-opening polymerization of 1,3,5-trimethyl-1,3,5-trivinylcyclotrisiloxane (ABCR, Germany), as described in ref 24. Its number average molecular weight (M_n) and molecular weight distribution (M_w/M_n) were equal to 6800 g/mol and 1.2, respectively, (GPC, methylene chloride,

polystyrene standards). The M_n value calculated based on the ^{1}H NMR spectrum was 6250 g/mol.

2,4,6,8-Tetramethylcyclotetrasiloxane (D_4^H), nonionic surfactant: dimethylsiloxane−ethylene glycol copolymer (DBE-224), and Karstedt's catalyst solution (2 wt % of Pt in xylene) were purchased from ABCR, Germany, and applied in the experiments as received. The solvents: THF and chlorobenzene were supplied by POCh, Poland and purified before use by standard procedures. The salts: NaCl and AgNO$_3$ were bought from POCh, Poland, while palladium(II) acetate [Pd(OAc)$_2$, 47 wt % of Pd]—from Aldrich; they were applied in the studies without any preliminary treatment.

2.2. Preparation of the V$_3$ Polymer-Based polyHIPEs. V$_3$ polymer-based polyHIPEs were prepared by cross-linking of the synthesized V$_3$ polymer (Section 2.1) with D$_4^H$ in HIPE using a modified procedure as compared to that described by Grosse et al. for PHMS.[19] HIPE preparation involved the formation of the continuous oil phase first. It was prepared by thorough mixing of the V$_3$ polymer, D$_4^H$, DBE-224, and chlorobenzene in an agate mortar. To the obtained mixture, under continuous stirring, the internal aqueous phase (0.02 M NaCl solution in water) was added drop-wise. Subsequently, to the resultant homogeneous emulsion, Karstedt's catalyst solution was introduced. Then, the emulsion was transferred into a Teflon crucible, placed in an oven and heated at 80 °C for 24 h. Monolithic materials obtained after this time were cut into small (few millimeters in each size) pieces, washed with THF/water (1:1 v/v) mixture, and filtered. Washing was repeated until no AgCl precipitation upon exposure of the filtrate to 1 M aqueous AgNO$_3$ solution occurred. Then, the materials were extracted with acetone in a Soxhlet apparatus for 6 h. Finally, the obtained materials were dried in air at room temperature.

In a typical cross-linking process, 1 g of the V$_3$ polymer was used, while the amounts of D$_4^H$ were changed in order to obtain molar ratios of Si−Vi groups (Vi denotes vinyl) from the polymer to Si−H groups from D$_4^H$ in the reactions with ratios equal to 1:0.44, 1:0.66, 1:1, and 1:1.5. The amounts of other HIPE components were as follows: DBE-224 constituted 20% of the sum of the V$_3$ polymer and D$_4^H$ weights, chlorobenzene—20% of the sum of the V$_3$ polymer, D$_4^H$ and DBE-224 weights, whereas NaCl solution constituted 82 vol % of the emulsion. In all reactions, 7 μL of the Karstedt's catalyst solution were used.

In the following sections, V$_3$ polymer-based polyHIPEs prepared at Si−Vi/Si−H molar ratios equal to 1:0.44, 1:0.66, 1:1, and 1:1.5 will be denoted V3_1:0.44, V3_1:0.66, V3_1:1, and V3_1:1.5, respectively.

2.3. Incorporation of Palladium into the V$_3$ Polymer-Based polyHIPEs. Palladium was incorporated into the prepared V$_3$ polymer-based polyHIPEs from the 4.7×10^{-3} M solution of Pd(OAc)$_2$ in THF using an appropriate volume of the solution to get 2 wt % of Pd in the resultant material. Before subjecting it to the Pd(OAc)$_2$ solution, the cross-linked polymer samples were crushed. Then, the suspensions were stirred at room temperature under an Ar atmosphere for 24 h, the polymer with incorporated Pd was separated from the solvent by centrifugation, washed several times with THF using a centrifuge, and dried on a vacuum line (pressure: 10^{-2} mbar).

Further on in this paper, the samples with incorporated palladium will be referred to as V3_1:0.44_Pd, V3_1:0.66_Pd,

V3_1:1_Pd, and V3_1:1.5_Pd, where the first part of the symbol stands for the polyHIPE serving as the matrix for Pd.

2.4. Characterization Methods. Equilibrium swelling of the prepared polyHIPEs was determined in THF. In the experiments, to the weighed amount of the studied sample, an excess of the solvent was added. After 48 h, the excess solvent was separated and the swollen sample was weighed. Swelling degrees reported in this work were calculated as $(m_s - m_0)/m_0$ ratios, where: m_s—weight of the swollen sample and m_0—weight of the sample subjected to swelling.

Skeletal density (d_{sk}) of the V$_3$ polymer-based polyHIPEs was measured using a Micromeritics AccuPyc II 1340 helium pycnometer. Apparent (bulk) density (d_{app}) was determined by weighing cuboids $5 \times 5 \times 4$ mm (length × breadth × height) in size cut from the samples. Total porosity of the prepared materials given in the work was calculated by the equation: $(d_{sk} - d_{ap}/d_{sk}) \times 100\%$.

Scanning electron microscopy (SEM) studies of the cross-linked polymer samples were conducted on an Ultra High-Resolution Scanning Electron Microscope Nova Nano Sem 200 (FEI EUROPE COMPANY). The materials of around $4 \times 4 \times 2$ mm in dimensions were attached to a sample holder using a graphite paste. Samples with introduced Pd were examined on a JEOL JSM-7500F scanning electron microscope equipped with a INCA PentaFetx3 EDS spectrometer. Powdered materials were placed on the conducting tape. In all SEM experiments, the investigated samples were sputtered with a carbon layer.

Transmission electron microscopy (TEM) investigations were performed on a Tecnai G2 FEG transmission electron microscope operating at 200 kV equipped with a high-angle annular dark-field scanning TEM detector (STEM−HAADF) coupled to the energy-dispersive X-ray (EDX) EDAX microanalysis system. Samples for TEM analyses were prepared by pouring a suspension of the examined material in ethanol onto a carbon film-coated copper grid, followed by evaporation of the solvent.

Fourier transform infrared−attenuated total reflection (FTIR−ATR) spectra were measured using a BIO-RAD Excalibur spectrometer. Spectra were collected after 64 scans. The resolution of the measurements was equal to 4 cm^{-1}. Quantitative analysis of the obtained spectra involved the calculations of the ratios of integral intensities of the bands at 2161 and 1258 cm^{-1}.[24] It was performed in the Origin Pro 2020 program after correction of spectra baselines.

Solid-state NMR spectra were recorded using a Bruker AVANCE III 500 MHz WB spectrometer operating at 11.7 T. For ^{29}Si MAS-NMR, the basic resonance frequency of 99.36 MHz was used. The samples were packed into 4 mm rotors and spun at 8 kHz during the examination. $\pi/3$ pulse (6.0 μs) and the repetition time of 31 s were used. Typically, 4200 scans were acquired. Deconvolutions of the spectra were performed using TopSpin 3.1 Bruker software. Chemical shifts were referenced to TMS.

X-ray photoelectron spectra (XPS) measurements were conducted on a Scanning XPS Microprobe PHI 5000 VersaProbe II (ULVAC-PHI, Chigasaki, Japan) equipped with a monochromatic Al Kα radiation source. The measured spectra were deconvoluted into mixed Gaussian/Lorentzian curves. Maxima positions were referenced to the C 1s line at binding energy (B.E.) equal to 284.8 eV.

Amounts of Pd in the samples were determined by energy-dispersive X-ray fluorescence (XRF) using a WD-XRF ZSX

Table 1. Characteristics of the V_3 Polymer-Based polyHIPEs Prepared in the Work

| sample | swelling degree [g/g] | density [g/cm^3] | | porosity [%] | SiH/SiCH$_3$ in FTIR spectra [%] | ^{29}Si MAS-NMR spectra analysis: shares of the signals [%][a] | | | |
		skeletal	apparent			V + D^H	D^c, (D^c calc.)[b]	D^{OH}	T
V3_1:0.44	8.1	1.0442 ± 0.0029	0.8806	20.1	-	66	34 (47.4)	-	-
V3_1:0.66	7.1	1.0388 ± 0.0050	0.0951	90.8	13.9	61	39 (57.2)	-	-
V3_1:1	5.7	1.0574 ± 0.0044	0.1052	90.0	40.0	50	43 (100)	1	6
V3_1:1.5	4.4	1.0685 ± 0.0049	0.0432	96.0	80.3	33	52 (100)	3	12

[a]Symbols denote: V—[SiO$_2$(CH$_3$)(CH=CH$_2$)] units, D^H—[SiO$_2$(CH$_3$)H] units, D^c—cross-linked i.e. [SiO$_2$(CH$_3$)(CH$_2$CH$_2$)] units, D^{OH}—[SiO$_2$(CH$_3$)OH] units, and T—[SiO$_3$(CH$_3$)] units (Table S1). [b]Brackets give hypothetical shares of the D^c signals in the spectra calculated with the assumption that all Si—H groups of D$_4^H$ added to HIPE took part in the hydrosilylation reaction.

Primus II Rigaku spectrometer. The analyses were performed for the pellets (30 mm in diameter) prepared from the mixture of the finely ground analyzed material, mixed with a cellulose-based binding agent. The results were based on the calibration curve obtained for palladium-containing polysiloxane materials using Pd(OAc)$_2$ as the Pd source.

X-ray diffraction studies were carried out on a PANalytical Empyrean diffractometer equipped with a semiconductor detector; Cu Kα (λ = 1.54 Å) radiation was used. The primary beam setup consisted of the focusing mirror and 1/32° molybdenum divergence slit. All measurements were carried out at room temperature and under ambient pressure. Based on the recorded diffractograms, mean sizes of Pd crystallites present in the samples were calculated by applying Scherrer equation to the Pd(111) peak after its mathematical fitting in the HighScore Plus program.

A gas chromatograph (Clarus 500, PerkinElmer) with He as the carrier gas (flow rate 1 cm^3/min) equipped with a capillary column Elite 5MS (0.25 mm × 0.25 mm × 30 m) and a flame ionization detector was used for analyzing the reaction mixture after catalysis.

2.5. Catalytic Experiments. Hydrogenation experiments were carried out in an agitated batch glass reactor under atmospheric pressure of hydrogen and at room temperature following the previous methodology.[35,36] The following operating conditions were applied: first, 50 mg of the Pd-containing material, placed in a flask, were sonicated for 15 min in 20 cm^3 of THF (freshly distilled) to ensure good dispersion of the catalyst in the solvent. Then, the mixture was transferred into a glass reactor affixed to a platform shaker and another 20 cm^3 of THF were added to it. Subsequently, the catalyst was flushed with N$_2$ and activated by passing H$_2$ through the reactor for 20 min at room temperature with gentle shaking. After activation, 200 μL of PhAc were introduced and the hydrogenation reaction began. Liquid samples were withdrawn from the reactor using a syringe at appropriate intervals of time and analyzed by gas chromatography. The PhAc, styrene, and ethylbenzene contents in the reaction mixtures were determined by comparison with calibration curves using n-decane as an external standard.

Shaking of a reactor was carried out at such a speed to ensure that the reaction rate did not depend on agitation speed.

Throughout the experiments, only styrene and ethylbenzene formation was observed. The blank test carried out without H$_2$ passage tested negative for any reaction products which indicated that no Si—H involving hydrogenation occurred. Additionally, no products were observed when the tests were performed using V$_3$ polymer-based materials before Pd incorporation.

3. RESULTS AND DISCUSSION

3.1. Characterization of the V_3 Polymer-Based polyHIPEs. PolyHIPEs studied in this work were obtained by cross-linking of a given amount of the V$_3$ polymer (typically 1 g) with various amounts of D$_4^H$ in w/o HIPE containing 82 vol % of the aqueous phase (Section 2.2). Final products of all the reactions were white, monolithic solids. Differences, however, could be observed in the HIPE preparation step. Formulation with a low amount of D$_4^H$ (V3_1:0.44) became a homogeneous emulsion of low, milk-like viscosity only after ca. 10 min careful mixing with NaCl aqueous solution added dropwise, whereas the other ones, with higher amounts of D$_4^H$, required a significantly shorter time (ca. 4 min) to turn into viscous, homogeneous emulsions.

Obviously, changes in the amounts of D$_4^H$ used in the experiments must have resulted in various cross-linking degrees of the V$_3$ polymer. Moreover, the amount of cross-linker added to HIPE must have also influenced the rate of polymer cross-linking. Both these factors are of crucial importance for the microstructure of the polymer network formed in HIPE conditions. In order to obtain a porous material, due to instability of HIPE, the polymer cross-linking process should be sufficiently fast to occur before the emulsion collapses; the polymer cross-linking degree in turn should be high enough to prevent internal phase droplets from coalescing. Hence, the first goal of our investigations was to establish how the amount of D$_4^H$ present in the studied HIPE formulations affected the cross-linking level of the V$_3$ polymer, and then, how the polymer cross-linking level influenced the microstructure of the prepared materials.

Differences in cross-linking levels of the V$_3$ polymer in polyHIPEs prepared in the work were evaluated based on their equilibrium swelling in THF (Section 2.4). This method, even though some part of the solvent can be absorbed in the pores, has been applied to determine cross-linking degrees of polymers in organic polyHIPEs,[37] as indeed it is the cross-link density that governs swelling of polyHIPEs.[38] It was found that swelling degrees of polyHIPEs derived from the V$_3$ polymer decrease as the amount of the cross-linker in the reaction grows (Table 1). This indicates the expected relationship between the V$_3$ polymer cross-linking degrees in the systems, with the highest and the lowest ones in the V3_1:1.5 and the V3_1:0.44 materials synthesized using the highest and the lowest amounts of D$_4^H$, respectively. It is worth mentioning at this point that polyHIPEs prepared in this work swelled to higher degrees than the V$_3$ polymer-based nonporous networks studied by us previously, which may be partially explained, as already mentioned, by the sorption of the solvent in the pores. Interestingly, the lowest swelling degree out of the V$_3$ polymer-based polyHIPEs (4.4 g/g for the
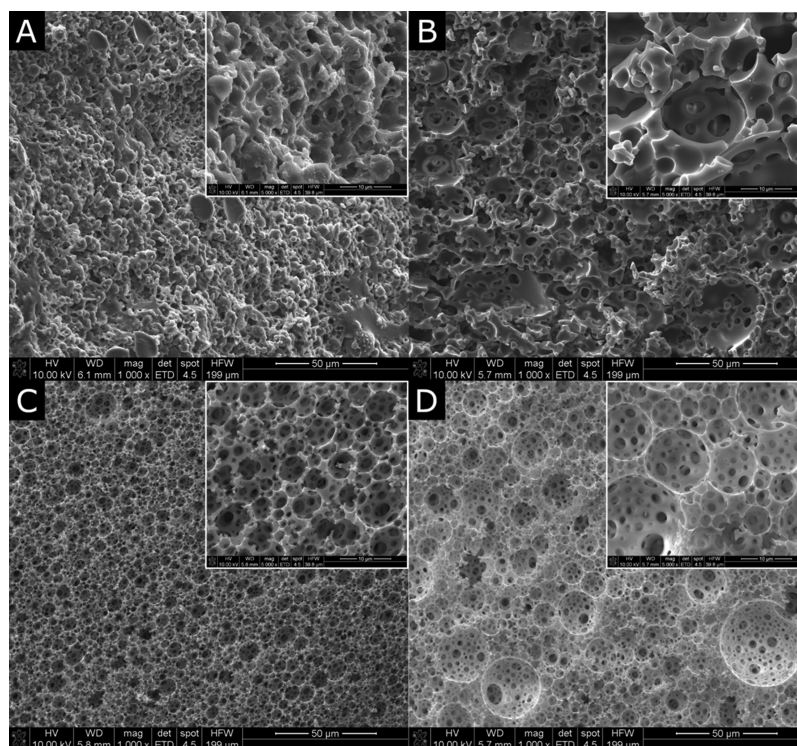
Figure 1. SEM images of polyHIPEs prepared in the work: (A) V3_1:0.44 material, (B) V3_1:0.66 material, (C) V3_1:1 material, and (D) V3_1:1.5 material.

V3_1:1.5 sample, Table 1) is quite close to that found for the nonporous material prepared by cross-linking of the dimethylsiloxane−V_3 block copolymer with D_4^H at the same reactive group molar ratio (3.98 g/g[28]). Because of the composition of its chain, in which the non-cross-linkable dimethylsiloxane segments constituted the major part (80%), the copolymer showed low cross-linking density. This suggests that cross-linking levels of the V_3 polymer in the studied polyHIPEs were also low.

The microstructure of the synthesized materials clearly depended on the amount of D_4^H added to HIPE, that is, on the V_3 polymer cross-linking degree. SEM images (Figure 1) show that only in the V3_1:1 and V3_1:1.5 samples, of higher polymer cross-linking levels, pore morphology typical of polyHIPEs[7−15,19] developed. In contrast, the V3_1:0.44 and V3_1:0.66 samples, of lower polymer cross-linking degrees, contained "flat", nonporous areas on their surfaces, more numerous in the case of the former than the latter one (Figure 1). This demonstrates that HIPEs in the V3_1:0.44 and V3_1:0.66 systems were unstable. Too low polymer cross-linking levels and/or too slow cross-linking process may have been the reasons for this. Instability of the V3_1:0.44 HIPE may have additionally arisen from, mentioned at the beginning of this section, its low viscosity which facilitated the mobility of the internal phase droplets in the emulsion making their coalescence easier. A similar phenomenon was postulated to occur during the preparation of organic polyHIPEs at higher temperatures, that is, in HIPEs of low viscosity.[39]

Although V3_1:1 and V3_1:1.5 materials, similarly to organic polyHIPEs, contained larger pores (often called voids[40]) interconnected by smaller ones (commonly referred to as windows[40]), their sizes were different in both systems (Figure 1). Spherical voids of diameter in the range between 2.6 and 10.5 μm were present in the V3_1:1, whereas the respective values were 2.6 and 41.0 μm for the V3_1:1.5 sample. Diameters of the windows, in turn, ranged from 0.3 to 3.2 μm in the case of the V3_1:1 and from 0.3 to 4.5 μm for the V3_1:1.5 material. Because voids reflect the dispersion of the internal phase in HIPE used to fabricate a polyHIPE, it can be concluded that aqueous phase droplets in the V3_1:1.5 emulsion were larger than in the V3_1:1 one.

Large voids in the V3_1:1.5 material of the highest V_3 polymer cross-linking level among the studied samples (Table 1) were rather unexpected. This is because growth in the void sizes with the increase in the polymer cross-linking degree is characteristic for polyHIPEs obtained in HIPEs stabilized by ionic and nonionic surfactants,[8] such as DBE-224 applied in this work. Possibly, however, attaining the final polymer cross-linking degree in this system was quite slow because D_4^H is a four-functional, cyclic compound, whose Si−H groups may have not reacted readily with vinyl groups of the polymer because of steric constraints. Thus, the aqueous phase droplets could have enlarged (most probably by Ostwald ripening) before the polymer reached the cross-linking level, resulting in its swelling degree established in the experiments.

The origin of windows in polyHIPEs is still controversial. It was proposed that they are generated because of the volume contraction of the continuous phase at the gel point.[41] According to other studies, they are formed during postsynthesis treatment of the materials.[42] Therefore, differences in the sizes of interconnections between voids in our polyHIPEs are difficult to rationalize and this point would require more investigations. Nevertheless, SEM images show that visibly more windows per one void were present in the V3_1:1.5 than in the V3_1:1 sample (Figure 1). Thus, the V3_1:1.5 polyHIPE exhibited a more interconnected porous structure than the V3_1:1 one.

The porous structure of the prepared materials was further characterized by density measurements. As can be seen in Table 1, apparent (bulk) density of most V_3 polymer-based polyHIPEs was in the range between 0.0432 and 0.1052 g/cm^3. Close values were reported for organic (0.056−0.067 g/cm^3[37]), PHMS-based (0.1−0.3 g/cm^3[19]), or silsesquioxane-containing (0.10−0.16,[21] 0.13−0.1822[22]) polyHIPEs. The V3_1:0.44 sample showed extremely high apparent density (0.8806 g/cm^3, Table 1) as compared with other materials, related to its lowest porosity revealed by SEM. Apart from V3_1:0.44, the total porosity of polyHIPEs fabricated in the work, calculated using apparent and skeletal densities (Section 2.4), varied from 90.8 to 96.0% (Table 1). Thus, it was higher than the internal phase content in the HIPEs applied in the preparation of these polyHIPEs (82 vol %, Section 2.2). A similar phenomenon observed for polyHIPEs derived from PHMS was attributed to the hydrolysis of some Si−H groups present in the polymer, which led to the evolution of hydrogen acting as a porogen.[19] Such an explanation does not seem to be valid in our V3_1:0.66 system, with a low amount of D_4^H, and consequently, low concentrations of Si−H groups. However, in view of ^{29}Si MAS-NMR studies discussed below, hydrogen must have been formed in V3_1:1 and V3_1:1.5 HIPEs. Additionally, the presence of chlorobenzene in our HIPEs (Section 2.2) may have contributed to high total porosity of our samples.

Finally, in order to determine their chemical composition, the synthesized polyHIPEs were examined using FTIR and ^{29}Si MAS-NMR spectroscopies (Section 2.4). All the recorded spectra confirmed the structure expected for the products of the V_3 polymer hydrosilylation with D_4^H. In particular, FTIR spectra (Figure 2) show the bands characteristic for:[24] Si−O
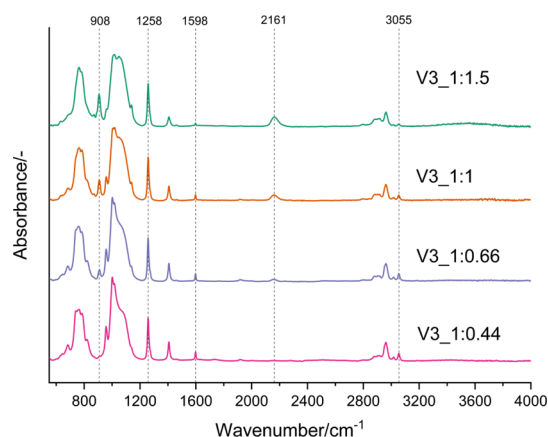

Figure 2. FTIR spectra of polyHIPEs prepared in the work.

bonds (1016, 1050 cm^{-1}), C−H bonds in −CH$_3$ groups (1258, 1408, 2905, 2960 cm^{-1}), as well as C−H bonds in −CH$_2$CH$_2$− bridges (1138 cm^{-1}) generated upon hydrosilylation. Additionally, not surprisingly because of the low V_3 polymer cross-linking degrees found for the prepared polyHIPEs, the bands originating from the reactive groups: vinyl (957, 1001, 1598, 3016, 3050 cm^{-1}) and Si−H (908, 2161 cm^{-1}) are also seen in the spectra. Intensities of the bands due to vinyl groups decrease as the amount of D_4^H used in the preparation of polyHIPEs increased, which is in line with the sequence of the growth in the cross-linking degree of the polymer in these materials. Intensities of the Si−H bands in the spectra change in the reverse order: they are the highest in

the spectrum of the V3_1:1.5 sample and practically not seen (apart from a weak shoulder at 908 cm^{-1}) in that of the V3_1:0.44 material (Figure 2) prepared using the highest and the lowest amounts of D_4^H, respectively. Such changes in intensities of the Si−H bands suggest that the fraction of these groups that stayed intact after the reaction in the systems grew as the amount of D_4^H used increased. This conclusion is corroborated by quantitative FTIR spectra analysis in which the ratios of the integral intensity of the band because of the Si−H group at 2161 cm^{-1} and that of the band ascribed to the C−H bonds in Si−CH$_3$ groups at 1258 cm^{-1} were calculated (Table 1).

All the measured ^{29}Si MAS-NMR spectra (Figure 3) contain two groups of signals: at chemical shift value, δ = ∼−35 ppm
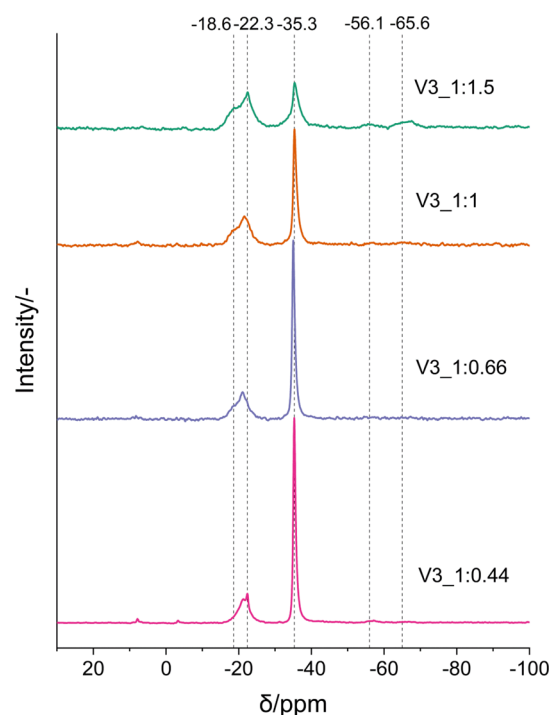
Figure 3. ^{29}Si MAS-NMR spectra of polyHIPEs prepared in the work.

and in the range of δ between −18 and −23 ppm. Because the V_3 polymer and D_4^H give rise to the maxima at −35.4 and −32.1 ppm, respectively,[43] the line at ∼−35 ppm in the spectra of polyHIPEs derived from the V_3 polymer should be treated as the superposition of the line corresponding to the [SiO$_2$(CH$_3$)(CH=CH$_2$)], that is, V units occurring in the polymer chain, and the one attributed to the [SiO$_2$(CH$_3$)H], that is, D^H units originating from D_4^H present in the materials (Table S1). Hence, this signal shows the existence of reactive groups that did not participate in the polymer cross-linking process in the studied polyHIPEs, found also by FTIR spectroscopy. Two overlapping maxima in the δ range between −18 and −23 ppm, in turn, can be attributed to the [SiO$_2$(CH$_3$)(CH$_2$CH$_2$)], that is, D^c units formed upon hydrosilylation, one present in the cross-linked polymer chain and the other in the ring structure being the part of the cross-linker (Table S1).[43] The share of the signal manifesting the presence of reactive groups in the systems, calculated after spectra decomposition, decreases and those of the signals because of the cross-linked units increase with the growing amount of D_4^H added to HIPE (Table 1), which is in

agreement with the sequence of the increase in the polymer cross-linking degree.

Based on the amounts of D_4^H applied in the reactions and assuming that all its Si−H groups participated in the hydrosilylation process, hypothetical shares of the signals corresponding to the cross-linked units (D^c) in the ^{29}Si MAS-NMR spectra were calculated (Table 1). Ratios of the experimental and calculated values can be used as a measure of the Si−H groups' conversion degrees during the preparation of V_3 polymer-based polyHIPEs in individual systems. They were as follows: 71.7, 68.2, 43, and 52% for the V3_1:0.44, V3_1:0.66, V3_1:1, and V3_1:1.5 samples, respectively.

In addition to the discussed signals present in the spectra of all studied polyHIPEs, the ^{29}Si MAS-NMR spectra of the V3_1:1 and V3_1:1.5 samples show the lines of low intensities at δ = ~−65 and ~−56 ppm (Figure 3). They are because of the $[SiO_3CH_3]$, that is, T, and $[SiO_2(CH_3)OH]$, that is, D^{OH} units of polysiloxanes, respectively.[44] These lines prove that during the preparation of V3_1:1 and V3_1:1.5 polyHIPEs, which involved the use of higher amounts of D_4^H than in the remaining systems, hydrolysis of some Si−H groups leading to silanol (Si−OH) moieties and their subsequent condensation resulting in T units took place. Both processes occurring in HIPE can modify the porous structure of polyHIPE formed, as they generate hydrogen (hydrolysis) and water (condensation). However, low shares of these signals in the spectra (Tables 1 and S1) suggest that in the studied systems hydrolysis and condensation reactions were not significant; their extent was higher in the V3_1:1.5 HIPE than in the V3_1:1 one. Therefore, it seems that their impact on the porous structure and porosity of the prepared materials, even though it cannot be excluded, was not very important.

3.2. Characterization of the V_3 Polymer-Based polyHIPEs with Incorporated Pd. Palladium was incorporated into the prepared polyHIPEs from 4.7×10^{-3} M Pd(OAc)$_2$ solution in THF using an appropriate volume of the solution to get 2 wt % of Pd in the obtained material (Section 2.3). THF is a good swelling solvent for V_3 polymer-based polyHIPEs (Table 1), which ensured accessibility of the bulk of the sample for the solution. However, we found that when the monolithic sample of a given polyHIPE was immersed in the Pd(OAc)$_2$ solution, the reaction (accompanied by the change in the color of the reaction medium, i.e. easy to establish visually) was very slow. Therefore, in order to enhance the efficiency of the Pd incorporation process, we decided to stir reaction mixtures. Unfortunately, because of their rather poor mechanical properties, our initially monolithic polyHIPE materials after stirring became powders of irregular grain shapes and sizes. Because of this, finally all monoliths were crushed before treatment with the Pd(OAc)$_2$ solution.

Crushing of the monolithic polyHIPEs caused breaking of some voids and windows present in their structure but retained their overall morphology, and, of course, it was not capable of altering the cross-linking levels of the V_3 polymer forming the polyHIPEs. Hence, it could be assumed that relationships between porosities and V_3 polymer cross-linking degrees for the crushed polyHIPEs were the same as those for the monolithic ones (Section 3.1).

It was found that Pd contents in the prepared samples, determined by XRF (Section 2.4), were in the range between 1.086 ± 0.022 and 1.700 ± 0.051 wt % (Table 2). Hence, palladium uptake constituted from 54.3 to 85% of its amount

Table 2. Characteristics of the V_3 Polymer-Based polyHIPEs with Incorporated Pd and Their Catalytic Activity in PhAc Hydrogenation

sample	Pd content [wt %]	SiH/SiCH$_3$ in FTIR spectra [%][a]	^{29}Si MAS-NMR spectra analysis: shares of the signals [%]				PhAc conversion after 1 h [%]	mean size of Pd crystallites [nm][b]	PhAc hydrogenation[c] initial rate	
			V + D^H	D^c	D^{OH}	T			mol PhAc/min g cat $\times 10^{-4}$	mol PhAc/min g Pd $\times 10^{-2}$
V3_1:0.44_Pd	1.086 ± 0.033	-	66	34	-	-	62	7.8	3.36	3.08
V3_1:0.66_Pd	1.700 ± 0.051	0.9 (93.5)	52	37	6	5	63	8.1	3.70	2.17
V3_1:1_Pd	1.490 ± 0.045	32.2 (19.5)	45	44	4	3	27	5.6	1.36	0.91
V3_1:1.5_Pd	1.416 ± 0.042	58.9 (26.7)	28	53	4	15	60	4.9	3.74	2.63

[a]In brackets conversion degrees (in %) of Si−H groups during incorporation of Pd into the studied polyHIPEs are given. They were calculated based on FTIR spectra using the expression: 100 − [(SiH/SiCH$_3$ ratio in the spectrum of the Pd-containing polyHIPE/SiH/SiCH$_3$ ratio in the spectrum of the initial polyHIPE) × 100]. [b]Calculated based on Pd(111) peak in the XRD pattern using Scherrer equation. [c]Reaction conditions: 40 cm^3 THF, 0.00182 mol PhAc, 0.05 g catalyst.

initially present in the solution. Interestingly, the highest amount of Pd was incorporated into the V3_1:0.66 polyHIPE, which was not characterized by a typical morphology of the HIPE-templated material (Figure 1) but showed high porosity and relatively high swelling degree (Table 1), that is, a relatively low polymer cross-linking level. On the other hand, the lowest amount of Pd was introduced into the V3_1:0.44 material whose swelling degree was the highest among the prepared polyHIPEs (Table 1), that is, the polymer cross-linking degree in it was the lowest; it also exhibited the lowest total porosity (Table 1). V3_1:1_Pd and V3_1:1.5_Pd samples, obtained using the matrices of the typical polyHIPE morphology (Figure 1), high total porosity and higher V_3 polymer cross-linking levels than in the remaining materials (Table 1) contained intermediate amounts of Pd (Table 2). These results show that, as could have been expected, high porosity led to higher Pd loadings in the materials. Moreover, the highest Pd content in the V3_1:0.66_Pd sample indicates that a relatively low polymer cross-linking degree in this case was an additional advantage. However, the lowest Pd amount in the V3_1:0.44_Pd sample prepared from the V3_1:0.44 polyHIPE in which—in spite of low porosity, but because of the high swelling degree—good penetration of $Pd(OAc)_2$ solution was ensured, suggesting that Pd uptake by the materials was not merely a function of their porosity and polymer cross-linking level. It could have been supposed that interactions between Pd^{2+} ions from $Pd(OAc)_2$ and the prepared polyHIPEs played an equally important role.

Interactions between Pd^{2+} ions and the prepared polyHIPEs were investigated by comparison of the FTIR and ^{29}Si MAS-NMR spectra of the Pd-containing samples with those corresponding to the respective ones before Pd incorporation. Of particular interest were the spectroscopic features signifying the presence of Si−H groups in the systems since in our earlier work devoted to nonporous polysiloxane networks, these moieties were found to participate in the reactions with Pd^{2+} and Pt^{4+} ions.[28,29]

FTIR spectra of the polyHIPEs with incorporated Pd (Figure 4) contain the bands seen also in the spectra of the initial samples (Figure 2). However, differences in the intensities of the bands at 2161 and 908 cm^{-1}, corresponding to the vibrations of Si−H bonds, can be observed. These bands show slightly (V3_1:1_Pd and V3_1:1.5_Pd) and more distinctly (V3_1:0.66_Pd) lower intensities in the spectra of the Pd-containing materials than in those of the respective

Figure 4. FTIR spectra of polyHIPEs with incorporated Pd.

starting polyHIPEs. It is also worth noting that the shoulder at 908 cm^{-1} visible in the spectrum of the V3_1:0.44 (Figure 2) is no longer present in that of the V3_1:0.44_Pd sample (Figure 4). Thus, it can be concluded that, similarly to the nonporous polysiloxane networks,[28,29] interactions of the prepared polyHIPEs with Pd^{2+} ions involved transformations of Si−H groups.

Quantitative analysis of the measured FTIR spectra, based on band integral intensities (Section 2.4), revealed that in the course of Pd incorporation almost all (93.5%) Si−H groups of the V3_1:0.66 polyHIPE were consumed (Table 2). These fractions were significantly lower (19.5, 26.7%) in the case of V3_1:1 and V3_1:1.5 materials (Table 2). It should be reminded here that the V3_1:0.66 polyHIPE, due to lower amount of D_4^H applied in its preparation, contained a lower amount of Si−H groups than the V3_1:1 and V3_1:1.5 ones (Section 3.1). Simultaneously, Pd loading in the V3_1:0.66_Pd sample was the highest (Table 2). Thus, the incorporation of this high amount of Pd into the V3_1:0.66_Pd sample involved conversion of most of the V3_1:0.66 polyHIPE's Si−H moieties. Lower metal contents in the V3_1:1_Pd and V3_1:1.5_Pd materials in turn used much lower fractions of the Si−H groups existing in the respective initial systems. Consequently, the lowest loading of Pd in the V3_1:0.44_Pd sample may have been related to the lowest content of Si−H groups in the V3_1:0.44 polyHIPE (Section 3.1).

FTIR spectra show no changes in the positions or intensities of the bands due to vinyl groups (957, 1001, 1598, 3016, 3050 cm^{-1}) upon the incorporation of Pd into the starting polyHIPEs (Figure 4 vs Figure 2). Thus, FTIR spectroscopy indicates that vinyl groups did not take part in the reactions occurring in the systems.

^{29}Si-MAS NMR spectroscopy provided a deeper insight into the processes proceeding in the studied polyHIPEs upon the incorporation of Pd. Lower relative intensities of the signal at chemical shift value $\delta = \sim$−35 ppm and higher of those at $\delta = \sim$−56 and $\sim$−65 ppm are the most distinct differences between the spectra of the Pd-containing (Figure 5) and the respective starting samples (Figure 3). This effect is particularly evident in the case of the V3_1:1.5 polyHIPE which contained the highest amount of Si−H groups, whereas it is practically not seen for the V3_1:0.44 material of the lowest Si−H groups' content. In view of this as well as in view of FTIR results, the decrease in the relative intensity of the signal at $\delta = \sim$−35 ppm, which is the superposition of the lines corresponding to D^H and V units existing in the systems (Section 3.1), should be attributed to the transformations of Si−H and not vinyl groups. Growths in the intensities of the signals due to D^{OH} ($\delta = \sim$−56 ppm) and T ($\delta = \sim$−65 ppm) units prove in turn that silanol (Si−OH) moieties resulted from the processes; some of them condensed to give T units. According to quantitative ^{29}Si-MAS NMR spectra analysis, the shares of D^{OH} and T units, however, were not high and other units were still dominant in the Pd-containing materials (Tables 2 and S2) like in the starting ones (Tables 1 and S1). Nevertheless, the formation of Si−OH groups shows that in the conversions of Si−H moieties in the systems water took part. Although Pd incorporation into the prepared polyHIPEs was conducted under an Ar atmosphere (Section 2.3) during 24 h processes, some air from the environment could have got into the reaction media. In principle, water vapor present in air
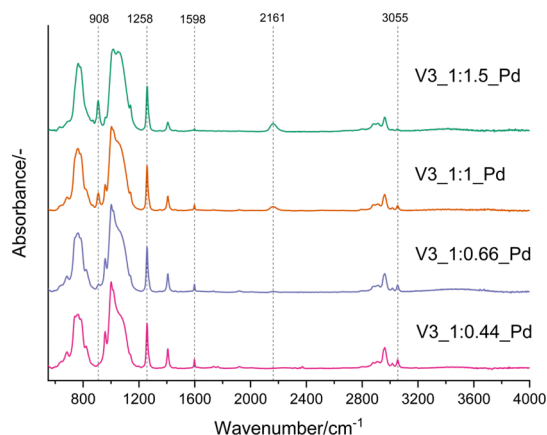
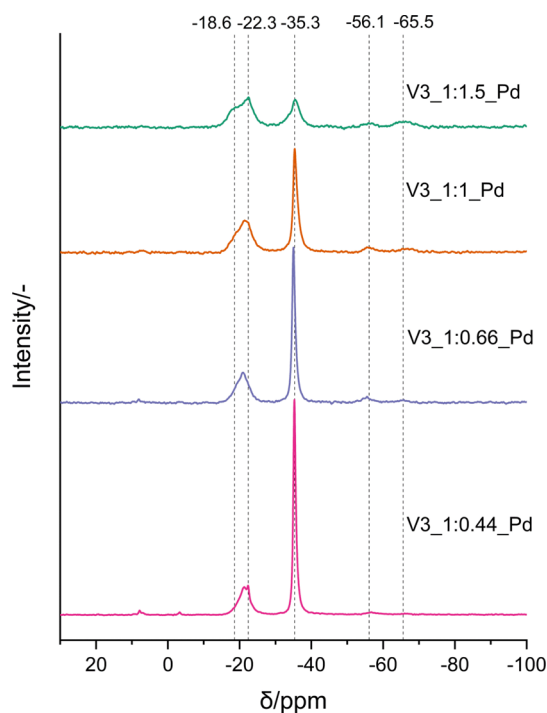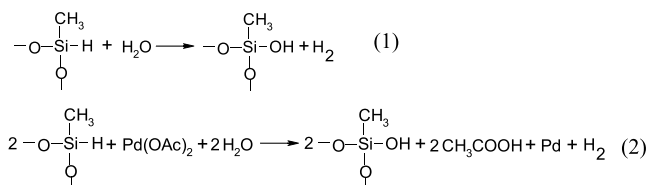**Figure 5.** ^{29}Si MAS-NMR spectra of polyHIPEs with incorporated Pd.

Figure 6. XRD patterns of polyHIPEs with incorporated Pd and fcc Pd standard (ICDD file 065-6174).

could have participated in two reactions generating Si−OH groups in the systems:

Reaction 1 was possible as Pd can be a catalyst of Si−H groups' hydrolysis. Reaction 1 in turn would result in the

$$-O-\underset{\underset{O}{|}}{\overset{\overset{CH_3}{|}}{Si}}-H + H_2O \longrightarrow -O-\underset{\underset{O}{|}}{\overset{\overset{CH_3}{|}}{Si}}-OH + H_2 \quad (1)$$

$$2-O-\underset{\underset{O}{|}}{\overset{\overset{CH_3}{|}}{Si}}-H + Pd(OAc)_2 + 2H_2O \longrightarrow 2-O-\underset{\underset{O}{|}}{\overset{\overset{CH_3}{|}}{Si}}-OH + 2CH_3COOH + Pd + H_2 \quad (2)$$

formation of metallic Pd observed by us previously in the nonporous polysiloxane networks.[28] Moreover, such a reaction is known to occur between Si−H groups and Pd^{2+} ions in aqueous solution.[45]

X-ray diffraction patterns (Figure 6) confirmed the presence of crystalline Pd in the synthesized samples, thus proving that the reduction of Pd^{2+} ions to metallic Pd, possibly by reaction 1, did proceed in our systems. The reflections at 2θ angle values of 39.9, 46.5, 68, 82.2, and 86.5° corresponding to (111), (200), (220), (311), and (222) planes, respectively, in the fcc crystalline lattice of Pd can be seen in the patterns of the Pd-containing samples. Additionally, the XRD patterns show broad maxima centered at $2\theta = \sim 12$ and $\sim 22°$ related to the amorphous cross-linked polysiloxane phase.[25]

As could be judged by the widths of the lines in the XRD 2θ angle region between 36 and 50° containing the most intensive Pd diffraction lines (inset in Figure 6), the sizes of Pd crystallites present in the samples differed significantly. This was corroborated by the calculations based on Pd(111) reflection by the Scherrer equation (Section 2.4): mean sizes of Pd crystallites were distinctly higher in two materials (V3_1:0.44_Pd and V3_1:0.66_Pd) obtained using poly-HIPEs of lower polymer cross-linking degrees and not showing a typical polyHIPE morphology than in the ones (V3_1:1_Pd

and V3_1:1.5_Pd) prepared from more cross-linked poly-HIPEs and of porous morphology characteristic for other polyHIPE materials (Table 2, Section 3.1). This shows that there was an influence of the polymer cross-linking degree and porous morphology on the sizes of Pd crystallites formed in the systems.

Similar differences in the sizes of Pd particles were revealed in SEM studies. Pd particles, represented by white spots, are clearly visible in BSE images of the V3_1:0.44_Pd and V3_1:0.66_Pd materials already at a magnification of 25,000 (Figure 7A,B); in the former one they are larger. On the other hand, in the other two samples, obtained using polyHIPEs of higher cross-linking degrees, Pd particles can be observed in BSE images only at magnifications as high as 100,000 (insets in Figure 7C,D), thus showing that the Pd nanoclusters existed in these samples, which is in agreement with the results of XRD studies.

It should be noted that Pd particles visible in BSE images were larger than the mean sizes of crystallites determined by XRD investigations. This demonstrates that Pd agglomerated in the systems. According to SEM, the largest agglomerates of diameter up to ca. 170 nm (0.17 μm) existed in the V3_1:0.44_Pd material. This was most probably because of its low porosity (Table 1) that facilitated the agglomeration of metal particles. In the case of the other samples of higher porosity (Table 1), Pd agglomerates were significantly smaller, their diameters did not exceed 30 nm. The presence of the areas with well-separated, uniform in size Pd particles in the V3_1:1.5_Pd specimen should be noted. This can be additionally related to the highest amount of Si−H groups in the V3_1:1.5 polyHIPE used for the preparation of this material, which shows that high concentration of Si−H groups
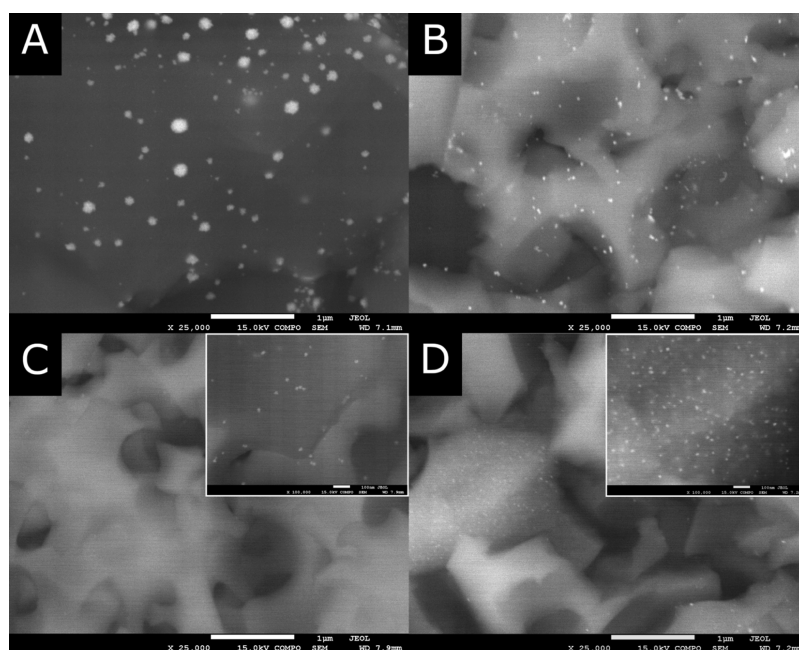
Figure 7. BSE images of polyHIPEs with incorporated Pd: (A) V3_1:0.44_Pd material, (B) V3_1:0.66_Pd material, (C) V3_1:1_Pd material, and (D) V3_1:1.5_Pd material.
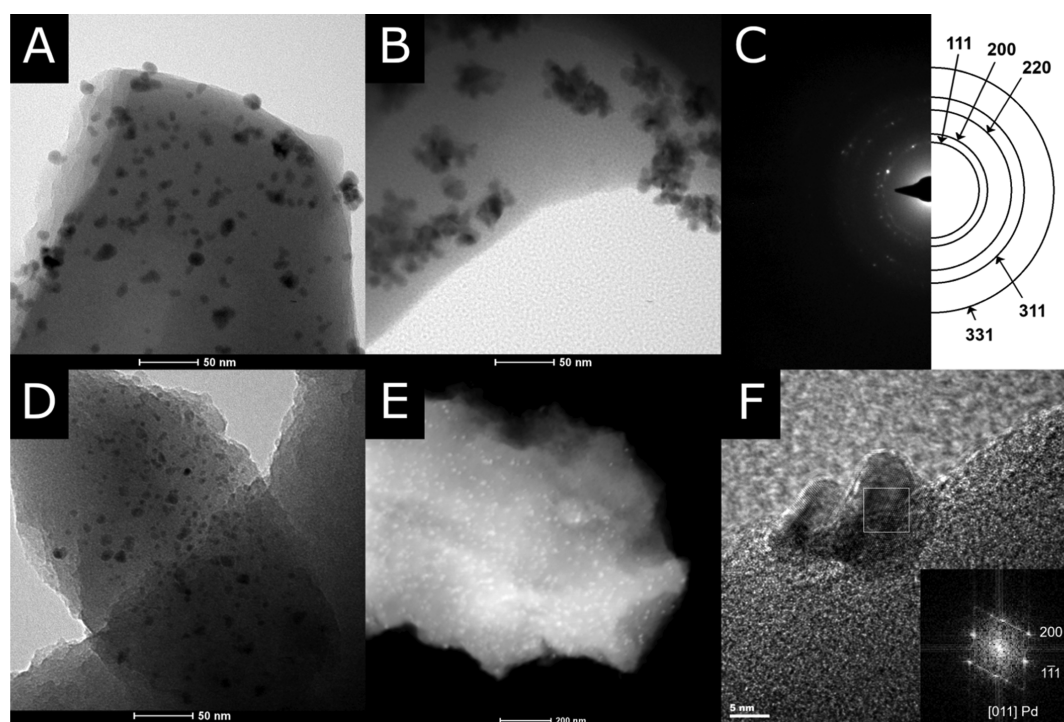

Figure 8. BF TEM images (A,B) and SAED pattern (C) of the V3_1:0.66_Pd sample; BF TEM (D), STEM−HAADF (E), and HRTEM with FFT (F) images of the V3_1:1.5_Pd sample.

is beneficial for achieving a good dispersion of metal particles within polyHIPE matrices derived from polysiloxanes.

V3_1:0.66_Pd and V3_1:1.5_Pd materials were additionally examined by TEM. Bright-field (BF) TEM images showed that both materials contained Pd nanoparticles whose diameter was in the range of 2.5−10 nm (Figure 8). Isolated Pd nanoparticles of a diameter below 10 nm were visible in high-resolution TEM (HRTEM) images of both specimens (Figure S1). Apart from nanoparticles, Pd agglomerates existed

in the samples, more and of larger sizes in the V3_1:0.66_Pd than in the V3_1:1.5_Pd one. They are seen in BF TEM (Figure 8) and STEM−HAADF (Figures 8, S2 and S3) images. EDX analysis conducted with a microscope operating in the STEM−HAADF mode showed that there were areas in which both, the polymer and Pd were present as well as the ones containing solely the polymer (Figures S2 and S3). It should be pointed out that all the described particles seen in the images corresponded to metallic Pd. This was established

based on the selected area electron diffraction (SAED) pattern (Figure 8) composed of reflections lying on the rings whose positions agreed with the interplanar distances in the fcc crystalline lattice of Pd reported in the literature (Table S3). Similarly, based on fast Fourier transform (FFT) obtained from the selected area marked in the HRTEM image, metallic Pd along the [011] zone axis could be identified (Figure 8). Most importantly, however, TEM supported the conclusion drawn from SEM studies that higher content of Si—H groups in the polyHIPE used for the incorporation of Pd inhibits agglomeration, that is, ensures better stabilization of metal particles.

To determine their surface chemical composition and to verify the surface oxidation state of Pd, XPS of selected samples with introduced metal particles were measured. The order of decrease in the surface Pd content established by XPS (V3_1:0.66_Pd > V3_1:1_Pd > V3_1:1.5_Pd, Table 3) is the

Table 3. Surface Composition of the Pd-Containing Samples Determined by XPS

	element contents [at %]				C/Si atomic ratio	O/Si atomic ratio
sample	Si	C	O	Pd		
V3_1:0.66_Pd	19.9	56.4	23.4	0.3	2.8	1.2
V3_1:1_Pd	21.7	52.8	25.3	0.2	2.4	1.2
V3_1:1.5_Pd	23.4	44.5	32.0	0.1	1.9	1.4

same as that found by bulk XRF analysis (Table 2). This is also the sequence of the decrease in C contents and increase in concentrations of Si and O on the surface of the samples detected by XPS (Table 3).

The relationships found by XPS for C and Si can be rationalized if one takes into account that the V$_3$ polymer contained three C atoms, while D$_4^H$—one C atom per one Si atom. Therefore, the cross-linking of the polymer with D$_4^H$ led to the decrease in the relative C amounts (C/Si atomic ratio) in the systems with respect to the starting polymer. Simultaneously, the relative amount of Si increased in this process. Thus, the results of XPS elemental analysis are consistent with the growth in the polymer cross-linking level in the prepared polyHIPEs, revealed also by other methods (Section 3.1).

Changes in O contents in the samples determined by XPS seem, in turn, to be connected with the formation of D^{OH} and T units in the materials upon the incorporation of Pd This is because the O/Si atomic ratios resulting from XPS analyses in all the cases were higher than 1 (Table 3), that is, the value expected for our perfect polysiloxane networks in which one O atom per one Si atom should have been present. The highest O/Si value observed for the V3_1:1.5_Pd sample of the highest D^{OH} + T unit content established by ^{29}Si MAS-NMR (Table 2) supports their contribution to this effect.

As illustrated in Figure 9, our measured high-resolution Pd 3d X-ray photoelectron spectra were characterized by the low signal to noise ratio. Therefore, their accurate decomposition was difficult and the obtained results should be treated as approximate. The spectra showed, however, the presence of metallic Pd (B.E. of Pd 3d$_{5/2}$ line in the Pd 3d$_{5/2-3/2}$ doublet equal to 335.5 eV) in the studied materials as well as the Pd(II) component (Pd 3d$_{5/2}$ maximum at ~337 eV) being the dominant one. The assignment of the latter doublet is not so
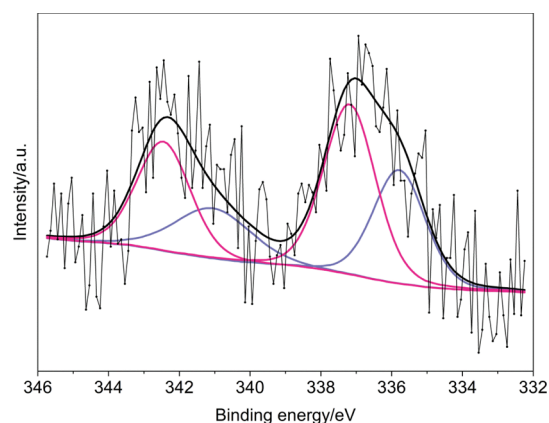

Figure 9. Pd 3d XPS of the V3_1:0.66_Pd sample.

straightforward. It is located in the B.E. region where the lines due to Pd in PdO may occur.[46] Hence, it may be due to surface oxidation in air of metallic Pd present in the systems. Such oxidation, however, usually manifests itself by the existence of up to 20% of the oxidized component in the Pd 3d X-ray photoelectron spectra. High shares of this Pd form in our spectra suggest that it can result from surface Pd-oxidation only in part. On the other hand, the Pd 3d$_{5/2}$ line at B.E. = 337.1 eV observed in the spectrum of Pd nanoparticles immobilized on MOFs and coated by a polydimethylsiloxane (PDMS) layer was ascribed to PdO$_x$ species and explained by the change in the electronic state of Pd nanoparticles after PDMS coating.[47] This indicates that the strong interactions between Pd and polysiloxane networks may exist, not detected in our studies. This problem would surely deserve more investigations, but they were beyond the scope of the present work.

3.3. Catalytic Properties of the Pd-Containing Systems. Hydrogenation of PhAc was selected as a probe reaction to compare catalytic properties of the studied samples. In this reaction, the C≡C bond in PhAc is hydrogenated to the C=C bond in styrene product, followed by subsequent hydrogenation to the C—C bond in ethylbenzene. On commonly studied inorganic carrier-supported Pd catalysts, the selectivity to the olefinic product is frequently reduced because of the formation of fully saturated product already in the stage of the C≡C bond hydrogenation. Catalysts of properties that make it possible to selectively obtain the product with the C=C bond in high yield are strongly desired.

It was observed that hydrogenation of PhAc occurred in the presence of all the prepared Pd-containing samples, whereas the Pd-free, initial polyHIPEs did not act as catalysts in this process. Thus, the catalytic activity was due to the presence of palladium in the tested samples.

The obtained plots of reagent concentration against reaction time are shown in Figure S4. The course of PhAc hydrogenation in the presence of the tested catalysts was similar to that observed over the Pd particles supported on other polymers,[35,36] with the concentration of PhAc diminishing, that of styrene passing through the maximum, and that of ethylbenzene increasing against reaction time. The V3_1:1_Pd catalyst was the exception as the hydrogenation process catalyzed by this material was slow and a maximum in styrene concentration was not reached within the conducted experiment.

The activity/selectivity patterns of tested catalysts are compared in Figure 10. The plots showing the decrease of
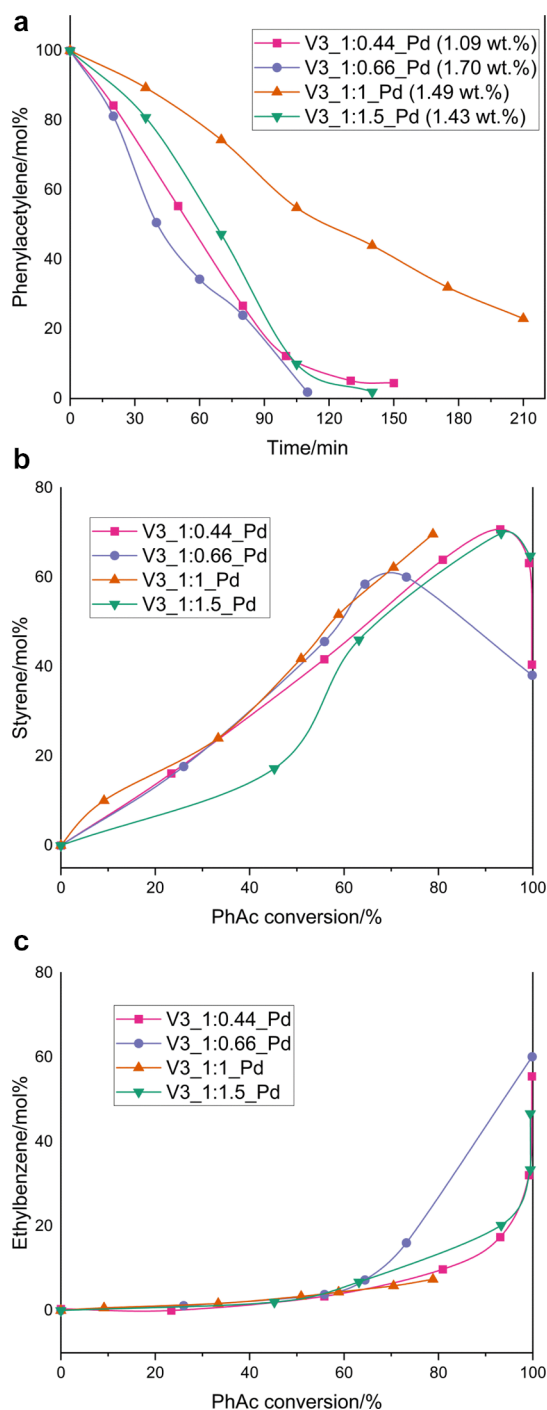

Figure 10. Results of hydrogenation of PhAc in the presence of polyHIPEs with incorporated Pd.

PhAc content against reaction time (Figure 10A) are close over studied catalysts, except for the least active V3_1:1_Pd one. In the presence of these three catalysts, the PhAc conversion degrees obtained after 1 h of the hydrogenation test are similar, 60–63% (Table 2) and the complete PhAc hydrogenation is reached after ca. 100 min of the reaction. The calculated initial rates of hydrogenation referred to 1 g of the catalyst are close, 3.36 to 3.74×10^{-4} mol PhAc/min·g (Table 2).

The initial hydrogenation rate referred to the total palladium content varies (Table 2). The highest rate (3.08×10^{-2} mol PhAc/min·g Pd) can be seen for the V3_1:0.44_Pd catalyst with large Pd particles (7.8 nm, Table 2) and the lowest polymer cross-linking degree (Table 1). The well-dispersed Pd nanoparticles (4.9 nm, Table 2) throughout the polymer of the high cross-linking degree in the V3_1:1.5_Pd system provide only a somewhat lower hydrogenation rate (2.63×10^{-2} mol PhAc/min g Pd). The materials have different palladium loadings (1.09−1.7 wt % Pd) as well as the Pd metal crystallites are determined by XRD to be of different average sizes (4.9−8.1 nm). In addition, the XRD diffraction patterns (Figure 6) indicate a remarkably smaller amount of the crystalline Pd in the V3_1:1_Pd than in the other three samples. This relation can be also seen by comparison of SEM images of the Pd-containing materials (Figure 7). SEM images of the V3_1:1_Pd sample (Figure 7C) show a definitively lower "density" of white spots representing the Pd metal particles than in the other materials. It seems, therefore, that the lowest rate of PhAc hydrogenation observed over the V3_1:1_Pd sample is the result of the lowest amount of metallic Pd in this material.

Over all the studied catalysts, the formation of styrene product dominates strongly (Figure 10B), whereas the product with the saturated C−C bond, ethylbenzene is formed in a very low concentration of ca. 5−6 mol % up to the PhAc conversion of ca. 80% (Figure 10C). Consequently, the obtained maximum concentrations of styrene are high (ca. 70 mol %) and they are reached at high PhAc conversion, ca. 90−93% (Figure 10B).

It can be also observed (Figure 10B) that the same maximum concentrations of styrene were reached over the V3_1:0.44_Pd and V3_1:1.5_Pd catalysts, with different properties of both the Pd phase (loading, metal particle size) and the polymer matrix. The former was characterized by the lowest polymer cross-linking degree (Table 1) and relatively large Pd particles (Figure 7A), whereas the well-dispersed Pd nanoparticles within the polymer matrix of the highest polymer cross-linking degree were observed in the latter catalyst (Figure 7D).

Activity/selectivity of Pd catalysts in hydrogenation of alkyne reagents has been commonly related to the electronic and/or morphological properties of the metal particles. High selectivity to alkene is related to its weak adsorption on metallic centers relative to that of alkyne, being the result of numerous factors, among them metal particle size and morphology.[48] In the case of polymer-supported catalysts, the influence of polymer network in the vicinity of catalytically active centers has been also taken into consideration.[36,49] Thus, similar activity of the studied catalysts accompanied by highly selective formation of styrene because of effectively inhibited its subsequent saturation to give ethylbenzene seems to be related to an influence of the polymer on the accessibility to the palladium active sites located inside the polymer network.

As described in the experimental part (Section 2.5), to ensure good dispersion of the catalyst in the reaction medium the Pd-containing samples were sonicated for 15 min in 20 cm³ of THF before the catalytic test. This resulted in finely dispersed catalyst particles whose separation after the catalytic test to perform recycling activity measurements appeared to be a difficult task, practically impossible. Porosity of the sonicated materials was not determined, and therefore, it is not possible

to conclude on the influence of their porosity on catalytic activity. However, it was observed that organic polyHIPEs with incorporated Pd particles showed higher catalytic activity after grinding than in the monolithic form.[31,32] It is possible that the powdered form would be the preferred one also for the catalytic applications of V₃ polymer-based polyHIPEs containing Pd.

4. CONCLUSIONS

In the work, macroporous polysiloxane materials (polyHIPEs) prepared by cross-linking of poly(methylvinylsiloxane) with a cyclic methylhydrosiloxane, D_4^H in w/o HIPE are described. Results of the studies allow concluding that:

(1) Total porosity and pore morphology of these systems depend on the polymer cross-linking degree. Higher polymer cross-linking degrees favor the formation of highly porous materials showing a typical polyHIPE open porous, interconnected microstructure.

(2) In the polyHIPEs of higher polymer cross-linking degrees, larger pores are formed which can be explained by the low rate of polymer cross-linking and enlargement of the internal phase droplets in HIPE before the end of the process.

(3) Polymer cross-linking degrees attained in the studied HIPEs are low, with reactive vinyl and Si—H groups preserved in the generated polyHIPEs.

(4) Treatment of poly(methylvinylsiloxane)-based poly-HIPEs with the $Pd(OAc)_2$ solution in THF results in the creation of metallic Pd particles. This process is accompanied by the transformations of Si—H groups remaining in the polymer network. Sizes of Pd crystallites are influenced by the polymer cross-linking degree in the polyHIPEs and thus by the porous morphology of polyHIPEs: they are smaller in the systems of higher polymer cross-linking levels, showing a typical polyHIPE microstructure.

(5) The Pd-containing materials are active catalysts in the hydrogenation of PhAc. Despite different metal loadings and sizes of Pd particles, the materials show similar activity and similar selectivity to styrene (80%) in this catalytic process. This can be explained by the influence of the polymer network on the accessibility of the palladium active sites for the reactants.

Results of the work can serve as general guidelines for the preparation of other polysiloxane-based polyHIPEs of an optimized porous structure in future and for their use as supports for new catalysts of various chemical processes or for other applications. Because of the advantageous properties of polysiloxanes, related to high stability of the Si—O bond, further studies on these topics are surely worthwhile.

ASSOCIATED CONTENT

Supporting Information

The Supporting Information is available free of charge at https://pubs.acs.org/doi/10.1021/acs.iecr.0c03429.

Analysis of ²⁹Si MAS-NMR spectra of V₃ polymer-based polyHIPEs prepared in the work; analysis of ²⁹Si MAS-NMR spectra of V₃ polymer-based polyHIPEs prepared in the work with incorporated Pd particles; HRTEM images of the: V3_1:0.66_Pd sample and V3_1:1.5_Pd sample; STEM−HAADF image of the V3_1:0.66_Pd sample and EDX spectra of the areas marked in the

image; STEM−HAADF image of the V3_1:1.5_Pd sample and EDX spectra of areas marked in the image; interplanar distances of Pd crystallographic planes determined by SAED in TEM studies and reported in the literature; and results of hydrogenation of PhAc in the presence of polyHIPEs with incorporated Pd (PDF)

AUTHOR INFORMATION

Corresponding Author

Magdalena Hasik − *Faculty of Materials Science and Ceramics, AGH-University of Science and Technology, 30-059 Kraków, Poland;* orcid.org/0000-0003-0911-0276; Email: mhasik@agh.edu.pl

Authors

Jan Mrówka − *Faculty of Materials Science and Ceramics, AGH-University of Science and Technology, 30-059 Kraków, Poland;* orcid.org/0000-0002-1419-6548

Mariusz Gackowski − *Jerzy Haber Institute of Catalysis and Surface Chemistry, Polish Academy of Sciences, 30-239 Kraków, Poland;* orcid.org/0000-0002-7131-9241

Lidia Lityńska-Dobrzyńska − *Institute of Metallurgy and Materials Science, Polish Academy of Sciences, 30-059 Kraków, Poland*

Andrzej Bernasik − *Faculty of Physics and Applied Computer Science, AGH-University of Science and Technology, 30-059 Kraków, Poland*

Robert Kosydar − *Jerzy Haber Institute of Catalysis and Surface Chemistry, Polish Academy of Sciences, 30-239 Kraków, Poland;* orcid.org/0000-0002-7666-9806

Alicja Drelinkiewicz − *Jerzy Haber Institute of Catalysis and Surface Chemistry, Polish Academy of Sciences, 30-239 Kraków, Poland;* orcid.org/0000-0001-7649-2118

Complete contact information is available at:
https://pubs.acs.org/10.1021/acs.iecr.0c03429

Notes

The authors declare no competing financial interest.

REFERENCES

(1) Florek, J.; Guillet-Nicolas, R.; Kleitz, F. Ordered Mesoporous Silica: synthesis and Applications. In *Functional Materials for Energy, Sustainable Development and Biomedical Sciences*; Leclerc, M., Gauvin, R., Eds.; DeGruyter: Berlin, Boston, 2014; pp 61−100.

(2) Hatton, B.; Landskron, K.; Whitnall, W.; Perovic, D.; Ozin, G. A. Past, Present and Future of Periodic Mesoporous Organosilicas—the PMOs. *Acc. Chem. Res.* **2005**, *38*, 305−312.

(3) Janiak, C.; Vieth, J. K. MOFs, MILs and more: concepts, properties and applications for porous coordination networks (PCNs). *New J. Chem.* **2010**, *34*, 2366−2388.

(4) Waller, P. J.; Gándara, F.; Yaghi, O. M. Chemistry of Covalent Organic Frameworks. *Acc. Chem. Res.* **2015**, *48*, 3053−3063.

(5) Wu, D.; Xu, F.; Sun, B.; Fu, R.; He, H.; Matyjaszewski, K. Design and Preparation of Porous Polymers. *Chem. Rev.* **2012**, *112*, 3959−4015.

(6) Barby, D.; Xia, Z. Low density porous cross-linked polymeric materials and their preparation and use as carriers for included liquids, EP0060138A1, 1982.

(7) Lépine, O.; Birot, M.; Deleuze, H. Influence of Emulsification Process on structure-properties relationship of highly concentrated reverse emulsion-derived materials. *Colloid Polym. Sci.* **2008**, *286*, 1273−1280.

(8) Zhang, S.; Chen, J. Synthesis of open porous emulsion-templated monoliths using cetyltrimethylammonium bromide. *Polymer* **2007**, *48*, 3021−3025.

(9) Zhang, S.; Chen, J.; Perchyonok, V. T. Stability of high internal phase emulsions with sole cationic surfactant and its tailoring morphology of porous polymers based on the emulsions. *Polymer* **2009**, *50*, 1723−1731.

(10) Li, C.; Jin, M.; Wan, D. Evolution of a Radical-Triggered Polymerizing High Internal Phase Emulsion into an Open-Cellular Monolith. *Macromol. Chem. Phys.* **2019**, *220*, 1900216.

(11) Sun, P.; Yang, S.; Sun, X.; Wang, Y.; Jia, Y.; Shang, P.; Tian, H.; Li, G.; Li, R.; Zhang, X.; Nie, C. Preparation of PolyHIPE Scaffolds for 3D Cell Culture and the Application in Cytotoxicity Evaluation of Cigarette Smoke. *Polymers* **2019**, *11*, 959.

(12) Utroša, P.; Ondr, O. C.; Žagar, E.; Kovačič, S.; Pahovnik, D. Shape Memory Behavior of Emulsion-Templated Poly(ε-Caprolactone) Synthesized by Organocatalyzed Ring-Opening Polymerization. *Macromolecules* **2019**, *52*, 9291−9298.

(13) Duan, C.; Zou, W.; Du, Z.; Li, H.; Zhang, C. Fabrication of micro-mesopores in macroporous (formaldehyde-melamine) monoliths via reaction-induced phase separation in high internal phase emulsion template. *Polymer* **2019**, *167*, 78−84.

(14) Kovačič, S. Ring Opening Metathesis Polymerization (ROMP) as a Tool for PolyHIPEs With Extraordinary Mechanical Properties. *Acta Chim. Slov.* **2013**, *60*, 448−454.

(15) Luo, Y.; Wang, A.-N.; Gao, X. Pushing the mechanical strength of PolyHIPEs up to theoretical limit through living radical polymerization. *Soft Matter* **2012**, *8*, 1824−1830.

(16) Zhang, H.; Zhao, R.; Pan, M.; Deng, J.; Wu, Y. Biobased, Porous Poly(high internal phase emulsions): Prepared from Biomass-Derived Vanilin and Laurinol and Applied as an Oil Adsorbent. *Ind. Eng. Chem. Res.* **2019**, *58*, 5533−5542.

(17) Gui, H.; Guan, G.; Zhang, T.; Guo, Q. Microphase-separated, hierarchical macroporous polyurethane from a nonaqueous emulsion-templted reactive block copolymer. *Chem. Eng. J.* **2019**, *365*, 369−377.

(18) Bai, X.; Dai, J.; Ma, Y.; Bian, W.; Pan, J. 2-(Allyloxy)methylol-12-crown-4 ether functionalized polymer brushes from porous PolyHIPE using UV-initiated surface polymerization for recognition and recovery of lithium. *Chem. Eng. J.* **2020**, *380*, 122386.

(19) Grosse, M.-T.; Lamotte, M.; Birot, M.; Deleuze, H. Preparation of Microcellular Polysiloxane Monoliths. *J. Polym. Sci., Part A: Polym. Chem.* **2008**, *46*, 21−32.

(20) Normatov, J.; Silverstein, M. S. Silsesquioxane-Cross-Linked Porous Nanocomposites Synthesized With High Internal Phase Emulsions. *Macromolecules* **2007**, *40*, 8329−8335.

(21) Normatov, J.; Silverstein, M. S. Interconnected Silsesquioxane-Organic Networks in Porous Nanocomposites Synthesized Within High Internal Phase Emulsions. *Chem. Mater.* **2008**, *20*, 1571−1577.

(22) Normatov, J.; Silverstein, M. S. Highly Porous Elastomer-Silsesquioxane Nanocomposites Synthesized Within High Internal Phase Emulsions. *J. Polym. Sci., Part A: Polym. Chem.* **2008**, *46*, 2357−2366.

(23) Nyczyk, A.; Paluszkiewicz, C.; Pyda, A.; Hasik, M. Preceramic Polysiloxane Networks Synthesized by Hydrosilylation of 1,3,5,7-tetravinyl-1,3,5,7-tetramethylcycloterasiloxane. *Spectrochim. Acta, Part A* **2011**, *79*, 801−808.

(24) Nyczyk, A.; Paluszkiewicz, C.; Hasik, M.; Cypryk, M.; Pospiech, P. Cross-linking of linear vinylpolysiloxanes by hydrosilylation - FTIR spectroscopic studies. *Vib. Spectrosc.* **2012**, *59*, 1−8.

(25) Wójcik-Bania, M.; Łącz, A.; Nyczyk-Malinowska, A.; Hasik, M. Polymethylhydrosiloxane networks of different structure and content of Si-H groups: Physicochemical properties and transformation into silicon oxycarbide ceramics. *Polymer* **2017**, *130*, 170−181.

(26) Olejarka, J.; Łącz, A.; Olejniczak, Z.; Hasik, M. Non-porous and porous materials prepared by cross-linking of polyhydromethylsilox-ane with silazane compounds. *Eur. Polym. J.* **2018**, *99*, 150−164.

(27) Chechelska-Noworyta, A.; Owińska, M.; Hasik, M. Hydrosilylation of nitrogen-containing compounds: model studies. *J. Organomet. Chem.* **2019**, *898*, 120866.

(28) Wójcik-Bania, M.; Olejarka, J.; Gumuła, T.; Łącz, A.; Hasik, M. Influence of Metallic Palladium on Thermal Properties of Polysiloxane Networks. *Polym. Degrad. Stab.* **2014**, *109*, 249−260.

(29) Wójcik-Bania, M.; Krowiak, A.; Strzezik, J.; Hasik, M. Pt supported on cross-linked poly(vinylsiloxanes) and SiCO ceramics - new materials for catalytic applications. *Mat. Des.* **2016**, *96*, 171−179.

(30) Munnik, P.; de Jongh, P. E.; de Jong, K. P. Recent Developments in the Synthesis of Supported Catalysts. *Chem. Rev.* **2015**, *115*, 6687−6718.

(31) Desforges, A.; Deleuze, H.; Mondain-Monval, O.; Backov, R. Palladium Nanoparticle Generation Within Microcellular Polymeric Foam and Size Dependence Under Synthetic Conditions. *Ind. Eng. Chem. Res.* **2005**, *44*, 8521−8529.

(32) Desforges, A.; Backov, R.; Deleuze, H.; Mondain-Monval, O. Generation of Palladium Nanoparticles Within Macrocellular Polymeric Supports: Application to the Heterogeneous Catalysis of the Suzuki-Miyaura Coupling Reaction. *Adv. Funct. Mater.* **2005**, *15*, 1689−1695.

(33) Ungureanu, S.; Birot, M.; Laurent, G.; Deleuze, H.; Babot, O.; Julián-López, B.; Achard, M.-F.; Popa, M. I.; Sanchez, C.; Backov, R. One-Pot Syntheses of the First Series of Emulsion Based Hierarchical Hybrid Organic-Inorganic Open-Cell Monoliths Possessing Tunable Functionality (Organo−Si(HIPE)) Series. *Chem. Mater.* **2007**, *19*, 5786−5796.

(34) Ungureanu, S.; Deleuze, H.; Sanchez, C.; Popa, M. I.; Backov, R. First Pd@Organo-Si(HIPE) Open-Cell Hybrid Monoliths Generation Offering Cycling Heck Catalysis Reactions. *Chem. Mater.* **2008**, *20*, 6494−6500.

(35) Drelinkiewicz, A.; Knapik, A.; Stanuch, W.; Sobczak, J.; Bukowska, A.; Bukowski, W. Diamine functionalized gel-type resin as a support for palladium catalysts: Preparation, characterization and catalytic properties in hydrogenation of alkynes. *React. Funct. Polym.* **2008**, *68*, 1652−1664.

(36) Drelinkiewicz, A.; Stanuch, W.; Knapik, A.; Ghanem, A.; Kosydar, R.; Bukowska, A.; Bukowski, W. Amine groups function-alized gel-type resin supported Pd catalysts: Physicochemical and catalytic properties in hydrogenation of alkynes. *J. Mol. Catal. A: Chem.* **2009**, *300*, 8−18.

(37) Rohm, K.; Manas-Zloczower, I.; Feke, D. Poly(HIPE) morphology, crosslink density, and mechanical properties influenced by surfactant concentration and composition. *Colloids Surf., A* **2019**, *583*, 123913.

(38) Kovačič, S.; Silverstein, M. S. Superabsorbent, High Porosity, PAMPS-Based Hydrogels through Emulsion Templating. *Macromol. Rapid Commun.* **2016**, *37*, 1814−1819.

(39) Carnachan, R. J.; Bokhari, M.; Przyborski, S. A.; Cameron, N. R. Tailoring the morphology of emulsion-templated porous polymers. *Soft Matter* **2006**, *2*, 608−616.

(40) Kimmins, S. D.; Cameron, N. R. Functional Porous Polymers By Emulsion Templating: Recent Advances. *Adv. Funct. Mater.* **2011**, *21*, 211−225.

(41) Cameron, N. R.; Sherrington, D. C.; Albiston, L.; Gregory, D. P. Study of the Formation of of the open-cellular morphology of poly(styrene/divinylbenzene) polyHIPE materials by cryoSEM. *Colloid Polym. Sci.* **1996**, *274*, 592−595.

(42) Menner, A.; Bismarck, A. New Evidence for the Mechanism of the Pore Formation in Polymerizing High Internal Phase Emulsions or Why PolyHIPEs Have an Interconnected Pore Network Structure. *Macromol. Symp.* **2006**, *242*, 19−24.

(43) Nyczyk-Malinowska, A.; Wójcik-Bania, M.; Gumuła, T.; Hasik, M.; Cypryk, M.; Olejniczak, Z. New precursors to SiCO ceramics derived from linear poly(vinylsiloxanes) of regular chain composition. *J. Eur. Ceram. Soc.* **2014**, *34*, 889−902.

(44) Marsmann, H. C. Silicon-29 NMR. *eMagRes*, Online; Wiley, 2011.

(45) Li, N.; Du, J.; Xu, L.; Xu, J.; Chen, T.-H. Facile fabrication of hollow hydridosilica nanoparticles with mesoporous shell and their dual effect in Pd nanoparticles immobilization. *Chem. Eng. J.* **2014**, *240*, 161−168.

(46) NIST X-ray Photoelectron Spectroscopy Database. *NIST Standard Reference Database Number 20*; National Institute of Standards and Technology: Gaithersburg MD, 20899, 2000.

(47) Li, H.; Zhao, W.; Fang, Z. Hydrophobic Pd nanocatalysts for one-pot and high-yield production of liquid furanic biofuels at low temperatures. *Appl. Catal., B* **2017**, *215*, 18−27.

(48) Molnár, A.; Sárkány, A.; Varga, M. Hydrogenation of carbon-carbon multiple bonds: chemo-, regio- and stereoselectivity. *J. Mol. Catal. A: Chem.* **2001**, *173*, 185−221.

(49) Corain, B.; Kralik, M. Dispersing metal nanoclusters inside functional resins: scope and catalytic prospects. *J. Mol. Catal. A: Chem.* **2000**, *159*, 153−162.